Numerical modeling of a magnetic-boiling based induced pump for thermal energy transport

SAJJAD AHANGAR ZONOUZI[1, *]

[1] *Department of Mechanical Engineering, Ilam University, Ilam, Iran*
[*] *Corresponding author email: s.ahangar@ilam.ac.ir*

Manuscript received 16 February, 2023; revised 02 March, 2023; accepted 03 March, 2023. Paper no. JEMT-2302-1433.

In the current study, a magnetic-boiling driven heat transport device has been introduced and modeled numerically. The numerical modeling of the problem has been carried out using Eulerian-Eulerian two phase model and control volume technique. The numerical results showed that a flow of magnetic nanofluid can be induced and drove inside a horizontal tube in the existence of magnetic field (MF) which is due to variations made in the magnetization of the ferrofluid by generation of the vapor bubbles during boiling process. The obtained results also showed that the simulated heat transport device powered based on magnetic-boiling induction is not only able to pump the ferrofluid through the tube, but also is able to transfer a considerable amount of heat generated in the electronic chip (heat source) as well. Furthermore, the flow rate of the induced flow inside the tube increases as the heat input of the heat source is increased. The heat source can be due to existence of a high heat flux electronic chip and the chip temperature (wall of the heated region) remains nearly unchanged during the flow boiling process in the heated region. The proposed magnetic- boiling driven heat transport device is usable in a closed circulating loop which can be extensively utilized in electronics cooling applications.

keywords: *Magnetic Field, Induced Pump, Boiling, Magnetic Nanofluid, Numerical Modeling.*

http://dx.doi.org/10.22109/JEMT.2023.385262.1433

NOMENCLATURE

A_Q	wall fraction affected by nucleating bubbles
c_p	specific heat $(J/Kg.K)$
d	diameter of the tube $(2mm)$
d_b	bubble mean diameter (m)
d_bw	bubble departure diameter (m)
f	frequency $(1/s)$
$\overrightarrow{F}_d$	drag force (N)
$\overrightarrow{F}_l$	lift force (N)
$\overrightarrow{F}_{wl}$	wall lubrication force (N)
N_a	density of active nucleation site $(1/m^2)$
q_T	total heat flux (W/m^2)
q_Q	quenching heat flux (W/m^2)
q_c	single-phase convective heat flux (W/m^2)
q_E	evaporation heat flux (W/m^2)
$\ddot{q}$	heat flux, (W/m^2)
T	temperature
T_c	curie temperature
$\overrightarrow{v}$	velocity (m/s)
$\overrightarrow{F}_{td}$	turbulent dispersion force (N)
$\overrightarrow{F}_{vm}$	virtual mass force (N)
$\overrightarrow{H}$	magnetic field vector (A/m)
g	gravitational acceleration(=-9.81 m/s^2)
h	heat transfer coefficient (W/m^2K)
H_{lv}	specific enthalpies difference (J/Kg)
h_c	liquid single-phase htc (W/m^2K)
k	thermal conductivity (W/mK)
k_B	Boltzmann constant
L	length $(60mm)$
L_f	Langevin function
M	magnetization (A/m)
M_s	saturation magnetization (A/m)
m_p	particle magnetic moment $(Am^2$)
Nu	Nusselt number, hd/k
N_a	density of active nucleation site $(1/m^2)$
q_T	total heat flux (W/m^2)

Greek symbols

χ	magnetic susceptibility

α void fraction
ρ density (kg/m^3)
μ dynamic viscosity ($kg/m.s$)
ζ parameter of Langevin
μ_B Bohr magneton

Subscripts

b bubble
b liquid
v vapor
w wall

1. INTRODUCTION

Magnetic nanofluids have the ability to be pumped in the existence of magnetic field (MF). Changing the magnetization of the ferrofluids with different techniques is a method which can be used in order to pump the ferrofluid in the presence of MF. One of the techniques for changing the magnetization of the ferrofluid is generation of vapor bubbles by boiling of them which results in decrease of magnetization. Such a magnetic-boiling driven heat transport device could be useful for providing cooling in hazardous environments and it can be used to transport microfluidic samples without contaminating theses samples. Moreover, the considered pump requires no mechanical or moving part.

The ferrofluids that are magnetically pumped have been investigated by some researchers. Iwamoto et al. [1] experimentally measured the force generated by a thermomagnetic pump for various rates of heat transfer and different tube inclinations. Karimi-Moghaddam et al. [2] studied the single phase ferrofluid flow inside a thermomagnetic loop. They considered a model for the magnetization of the ferrofluid and presented a correlation for heat transfer. Kamiyama et al. [3] studied the influence of boiling two-phase flow exposed to MF experimentally. They found that the boiling gas-bubbles effectively increases the magnetic driving force which is applied to the temperature sensitive magnetic fluid. Yang et al. [4] experimentally investigated the sub-millimeter thermomagnetic pumps with temperature-sensitive magnetic fluid. They achieved the highest flow rate of 81.74 l/min under the highest heating condition of 459.8 kW/m2. Pattanaik et al. [5] presented a self-regulating multi-torus magneto-fluidic device for kilowatt level cooling and they used a suitably imposed temperature and magnetic field gradients to drive ferrofluid in a 2 mm diameter glass capillary tube, without application of any external pressure gradient.

The purpose of the present work is presenting and numerical modeling of a heat transport device working based on magnetic-boiling induction which can transfer a considerable heat from the heat source. In fact, the present magnetic-boiling based pump represents a novel pumping system that can be operated by simply boiling and applying an external magnetic field. The heat source can be due to existence of a high heat flux electronic chip. The working fluid of the pump is a magnetic nanofluid. A MF resulted from a solenoid accompanied by variations made in the magnetization of the ferrofluid are used to induce and pump the ferrofluid inside a tube. The variations in the magnetization of the ferrofluid are made by generation of vapor bubbles due to boiling process. The mentioned pump will be numerically simulated using the technique of control volume and wall boiling model. According to the author' knowledge, there is no published paper in the literature about numerical modeling of the present problem. Besides, the proposed magnetic- boiling driven heat transport device is usable in a closed circulating loop which can be extensively utilized in electronics cooling applications.

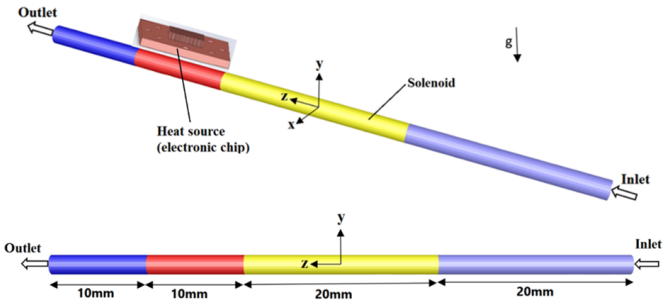

Fig. 1. Schematics of the studied magnetic-boiling driven heat transport device: (a) 3D view, (b) dimensions

Table 1. Properties of the used magnetic nanofluid.

density (kg/m^3)	dynamic viscosity (Pa.s)	thermal conductivity (W/mK)	specific heat (J/kgK)
1059.94	0.0007705	0.941	4115.26

2. PROBLEM DESCRIPTION

Fig. 1 shows the schematics of the studied magnetic-boiling driven device. The pump includes a tube with diameter of 2mm and length of 60mm filled with magnetic nanofluid. The tube has been placed horizontally. As seen, an electromagnetic solenoid with the length of 10mm mounted to the tube and it is used to make MF inside the tube. A heater (heat source) with the length of 20mm is located just after the solenoid and downstream of the solenoid. The heat source can be due to existence of a high heat flux electronic chip. The magnetic nanofluid is heated while passing the region where a heater is located and consequently, a gas liquid two phase flow is formed. The inlet subcooling of the ferrofluid has been considered as 8°C.

The studied magnetic nanofluid is a water based nanofluid with 2% volume fraction of iron oxide (Fe_3O_4) nanoparticles. The mean diameter of the nanoparticles is 10nm. In the present work, the effective thermal physical properties have been used and Table 1 shows the magnetic nanofluid's physical properties.

Moreover, the magnetization of the magnetic fluid is the function of void fraction and the temperature as follows [1].

$$M = \mu_0 \chi (1 - \alpha_v)(1 - \frac{T - T_0}{T_c - T_0})H \quad \textbf{(1)}$$

According to the above equation, the magnetization of the magnetic fluid in the heated region decreases as the gas bubbles appear and therefore, the value of the magnetization will be different before and after the location of the solenoid. It should be added that variations of the ferrofluid temperature is very low in the current problem and consequently, the effect of ferrofluid temperature variations on the magnetization values of ferrofluid is negligible. Thus, difference in the magnetization values before and after the location of the solenoid mainly originates from the formation of the gas bubbles in the heated region. In other words, the driving force due to the magnetization difference results from boiling of the magnetic fluid and occurrence of gas

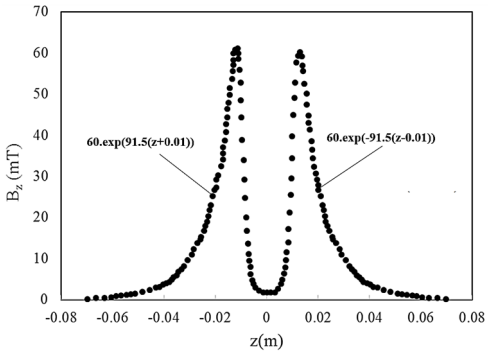

Fig. 2. MF distribution generated by solenoid [6]

bubbles which is accompanied by reduction of the magnetic fluid magnetization.

The used MF in this study for inducing flow inside the tube is resulted from an electromagnetic solenoid. Pal et al. [6] have used this MF experimentally in their thermomagnetic pump. Their used electromagnet (solenoid) consists 754 turns with electric current of 2.03A and they have presented the MF distribution created by this electromagnet both experimentally and numerically. Their obtained MF distribution has been depicted in Fig. 2 which will also be used in this study for applying MF to the ferrofluid inside the tube. As seen, the MF is non uniform in z direction. Moreover, since the diameter of the tube is very small in comparison with the length of the electromagnet, the gradient of the field in the radial direction is very small. It should also be added that since the tube is place horizontally, the natural convection driving force is negligible in comparison with the magnetic driving force.

3. GOVERNING EQUATIONS

The two phases considered in the governing equations are liquid ferrofluid and vapor ferrofluid. The equation of mass conservation for phase i is described by following equation [7, 8]:

$$\frac{\partial}{\partial t}(\alpha_i\rho_i) + \nabla.(\alpha_i\rho_i\overrightarrow{v_i}) = \dot{m}_i j - \dot{m}_j i \tag{2}$$

where ρ_i and $\vec{v}_i$ are the density and velocity vector of phase i respectively. The terms $\dot{m}_{ij}$ and $\dot{m}_{ji}$ are respectively the rate of mass transfer from phase i to j and j to i. Besides, the equation of momentum conservation for phase i is described by following equation[7]:

$$\frac{\partial}{\partial t}(\alpha_i\rho_i\vec{v}_i) + \nabla.\left(\alpha_i\rho_i\vec{v}_i\vec{v}_j\right) = -\alpha_i\nabla P + \nabla.\bar{\bar{\tau}}_i + \alpha_i\rho_i\vec{g} + \dot{m}_{ji}\vec{v}_j$$
$$-\dot{m}_{ij}\vec{v}_i + \left(\vec{F}_{drag,i} + \vec{F}_{lift,i} + \vec{F}_{wl,i} + \vec{F}_{td,i} + \vec{F}_{vm,i}\right) + \mu_0\left(\vec{M}.\nabla\right)\vec{H} \tag{3}$$

where $\bar{\bar{\tau}}_i$ denotes the tensor of stress-strain for the phase i. $\vec{F}_{drag,i}$ is the drag force and it is computed based on Ishi and Zuber [9], $\vec{F}_{lift,i}$ is the lift force and it is modeled using Tomiyama model [10]. Moreover, $\vec{F}_{wl,i}$, $\vec{F}_{td,i}$ and $\vec{F}_{vm,i}$ are also respectively wall lubrication force, turbulent dispersion force and virtual mass force which are modeled using Antal et al. [11], Burns et al. [12] and Zuber [13] respectively.

The term in Eq. Eq. (3), $\mu_0\left(\vec{M}.\nabla\right)\vec{H}$ denotes the magnetic force and M implies the magnetization which is calculated by following equation [1, 14, 15]:

$$M = M_s L(\xi)(1-\alpha_v)\left(1-\frac{T-T_0}{T_c-T_0}\right) = \frac{6\alpha_p m_p}{\pi d_p^3}\left(coth(\xi)-\frac{1}{\xi}\right)$$
$$\times(1-\alpha_v)\left(1-\frac{T-T_0}{T_c-T_0}\right) \tag{4}$$

In order to calculate the particle magnetic moment of the magnetic particles, the following formula is used:

$$m_p = \frac{4\mu_B\pi d_p^3}{6\times 91.25\times 10^{-30}} \tag{5}$$

Also, the parameter of Langevin ξ is as follows [16]:

$$\xi = \frac{\mu_0 m_p H}{k_B T} \tag{6}$$

An approximation for the Langevin equation is as follows [16]:

$$L(\xi) = \left(coth(\xi)-\frac{1}{\xi}\right) = \frac{1}{3}\frac{\mu_0 m_p H}{k_B T} \tag{7}$$

The magnetization can be considered as follows:

$$M = \frac{6\alpha_p m_p}{\pi d_p^3}\frac{1}{3}\frac{\mu_0 m_p H}{k_B T}(1-\alpha_v)\left(1-\frac{T-T_0}{T_c-T_0}\right) \tag{8}$$
$$= \mu_0\chi(1-\alpha_v)\left(1-\frac{T-T_0}{T_c-T_0}\right)H$$

The equation of energy conservation for phase i is given by the equation below [7, 17]:

$$\frac{\partial}{\partial t}(\alpha_i\rho_i h_i) + \nabla.(\alpha_i\rho_i\vec{v}_i h_i) = \alpha_i\frac{\partial P}{\partial t} - \nabla.\vec{q}_i + Q_{ij} + \dot{m}_{ji}h_j - \dot{m}_{ji}h_i \tag{9}$$

where h denotes the specific enthalpy, $\vec{q}_i$ is the vector of heat flux and Q_{ij} represents the term related to energy transfer between the phases.

A. Wall boiling model

The used model for modeling the flow boiling in the current investigation is RPI model proposed by Kurul and Podowski [18]. This model is based on the concept that heat from a wall to liquid is divided into three parts:

$$q_T = q_c + q_Q + q_E \tag{10}$$

where q_c is single-phase convective heat flux, q_Q denotes the quenching heat flux and q_E is related to the evaporation heat flux. The share of the heat flux due to single-phase convection can be calculated by the equation below:

$$q_c = (1-A_Q)h_c(T_w - T_l)(11) \tag{11}$$

where h_c denotes the single-phase heat transfer coefficient (htc). The net heat required for the formation of the vapor phase is names as evaporation heat flux and it is calculated as follows:

$$q_E = \frac{\pi}{6}{d_{bw}}^3 f N_a H_{lv} \tag{12}$$

where N_a is the density of nucleation sites, f is the frequency of the bubble detachment and d_{bw} is the departure diameter of the bubble. The quenching heat flux q_Q represents the heat transferred to the subcooled liquid from the bulk flow that fills

the volume vacated by departing bubbles. An analytical solution has been suggested by Del Valle and Kenning [19] for the quenching heat flux as follows:

$$A_Q = \min[1, N_a \pi {d_{bw}}^2] \tag{13}$$

$$q_Q = A_Q \frac{2K_l(T_w - T_l)}{\sqrt{\frac{\pi K_l}{f\rho_l c_{pl}}}} \tag{14}$$

Lemmert and Chawla [20] have represented a correlation for the density of nucleation sites which is dependent on wall superheat as follows:

$$N_a = (185\,(T_w - T_l))^{1.805} \tag{15}$$

Kurul and Podowski [21] also represented a correlation for the frequency of the bubble detachment as follows:

$$f = \sqrt{\frac{4g(\rho_l - \rho_v)}{3d_{bw}\rho_l}} \tag{16}$$

Modeling the subcooled nucleate boiling requires choosing the right bubble departure diameter. In the current work, the Tolubinsky and Kostanchuk correlation [22] is utilized:

$$d_{bw} = mindref.exp - TsubTref, dmax \tag{17}$$

where $d_{ref} = 0.6mm, Tref = 45K$ and $d_{max} = 1.4mm$.

B. Boundary conditions

Numerical modeling has been conducted using the steady-state condition in the present study. In the gas phase, the free slip boundary condition has been taken into account, and in the liquid phase, the no slip boundary condition has been taken into account. It has been applied a constant heat flux on a part of the wall of the tube where the heater (heat source) is located. Other parts of the wall of the tube have been considered as adiabatic. Moreover, at the inlet and outlet of the tube, the pressure boundary condition was implemented.

4. NUMERICAL METHOD

The technique of the volume control has been utilized to discretize the coupled differential equations. The SIMPLEC technique has also been implemented for velocity–pressure coupling. The used scheme to solve the convection- diffusion equations is second order upwind method. The eddy viscosity model developed by Sato's [23] has been used for turbulence viscosity calculations. The eddy viscosity model has been implemented for computation of the turbulence viscosity. The SST $k-\omega$ turbulence model has been used for modeling the continuous phase and it has been assumed that dispersed vapor is laminar. Structured grid is used to model the problem as depicted in in Fig. 3 and the number of the mesh used in this study is 25240. For ensuring that the results are independent from grid, several grid distributions have been examined. Table 2 shows the results of grid independency for the studied geometry. As seen, increasing the mesh numbers slightly changes the flow rate of the induced flow inside the tube for two different considered heat fluxes.

In order to validate the numerical method used in the current study, numerical htc values for water-Al2O3 nanofluid flow through a horizontal tube were compared with those from the experimental study of Kim et al. [24]. As seen in Fig. 4a, there is a good agreement between them. Moreover, to validate the

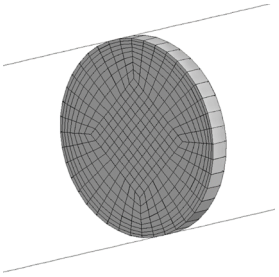

Fig. 3. Used grid

Table 2. Grid independency check for the induced flow rate for two different heat inputs.

heat input (W)	mesh numbers	v (ml/s)
2.01	17280	0.070076
2.01	25240	0.070765
2.01	32560	0.070977
2.51	17280	0.07451
2.51	25240	0.075617
2.51	32560	0.075884

numerical approach in the presence of MF, the obtained results from the present numerical approach have been compared with those presented by Bahiraei et al. [25] for variations of the distribution of velocity inside the inner tube of a double pipe heat exchanger consisting a ferrofluid with 4% volume fraction of nanoparticles which is exposed to a radial MF resulted from quadrupole MF with maximum strength of B0. The results have been presented in Fig. 4b and as seen, there is a good consistency between them. Besides, for validation of the accuracy of the boiling model used in the present study, the numerical results obtained by the boiling model (two fluid model) used in the present study have been compared with experimental data of Manon et al. [26, 27] for the subcooled flow boiling inside a vertical pipe having an inner diameter of 19.2 mm. The inlet temperature, working pressure, mass flux and the applied heat flux in their study were 341.8K, 2.62 MPa, 2000 kg/m2s and 75KW respectively and the working fluid was R-12. Fig. 4c and Fig. 4d compare the two fluid model results for gas phase velocity and void fraction with results of Manon et al. [26]. As seen, the results of the numerical analysis and the experimental analysis agree well.

5. NUMERICAL RESULTS AND DISCUSSION

First, it should be noted that the electric conductivity of the ferrofluid has been considered as negligible. Thus, the MHD force is neglected. Fig. 5 shows the directions of the magnetic forces due to the MF resulted from the solenoid. As the wall temperature of the heated region surpasses the magnetic nanofluid saturation temperature, the vapor bubbles and the gas phase will be formed in the heated region which contributes to reduction of magnetization and consequently reduction of the magnetic force in this region. The blue vectors shown in Fig. 5 depict the direction and magnitude of the magnetic force applied on the

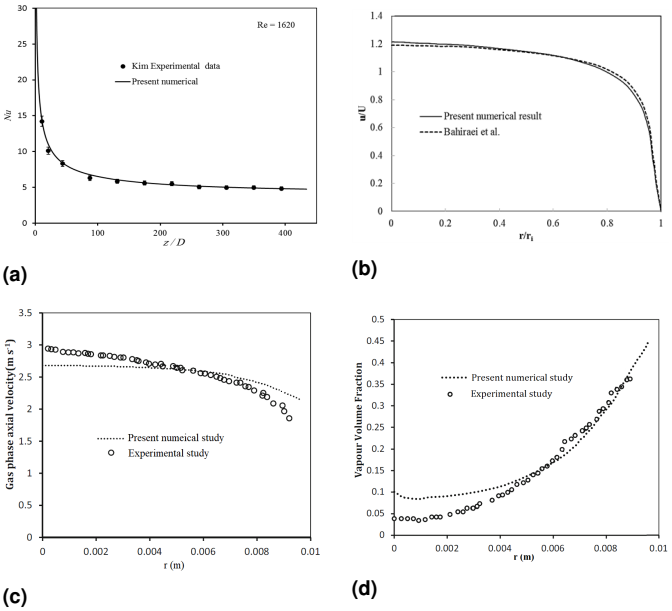

Fig. 4. Validation of the numerical results with a) results of Kim et al. [24] for the variations of Nusselt Number for water-Al2O3 nanofluid flow inside a horizontal tube, b) numerical approach of Bahiraei et al. [25] including a double pipe heat exchanger under radial MF, c) experimental results of Manon et al. [26] for gas phase velocity, d) experimental results of Manon et al. [26] for void fraction.

magnetic fluid in different regions, including the region before entering the solenoid, inside the solenoid, and the region after the solenoid (heated region). In the region before the solenoid, according to the distribution of the magnetic field resulting from the solenoid, the direction of the magnetic force is to the left, while in the heated region, the direction of the magnetic force is to the right. Another point is that due to the formation of bubbles in the heated area, the amount of magnetic force generated in this region is less than the magnetic force in the region before the solenoid, and consequently, the result of the magnetic forces in different regions around the solenoid will be to the left.

Fig. 6 shows variations of the induced flow through the tube by increasing heat input of the heat source. As seen, with increasing heat flux (heat input), the induced flow rate inside the tube increases. By increasing the heat flux, the volume fraction of vapors in the heated region increases and more bubble vapors

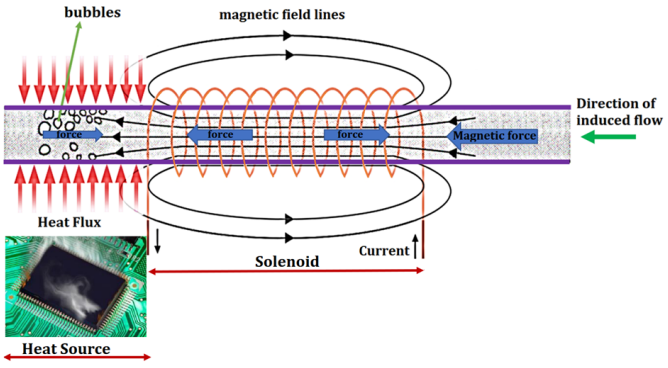

Fig. 5. Direction of the magnetic forces around the solenoid.

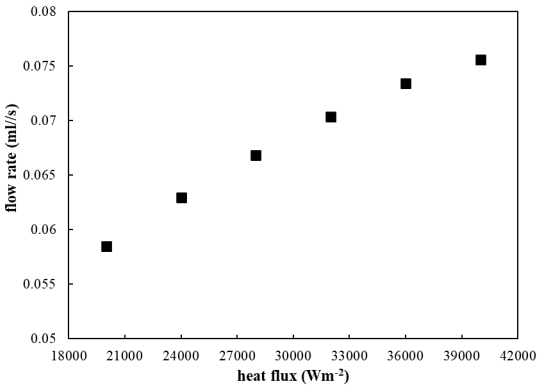

Fig. 6. Variations of the induced flow inside the tube in terms of the heat input in the heat source.

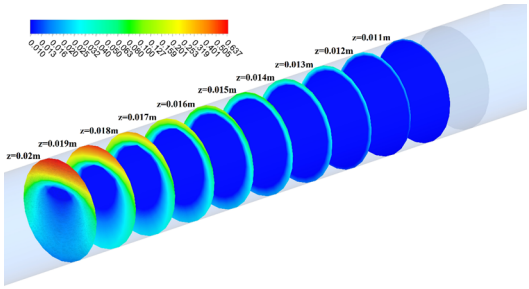

Fig. 7. Vapor volume fraction contour over the transversal cross sections for the heat input of 2.51W.

are generated which result in decrease of magnetization in the heated region and contributes to increase of driving force and consequently increase of the induced flow rate in the studied magnetic-boiling driven device.

Fig. 7 depicts the vapor volume fraction contour over the transversal cross sections of z=0.011, 0.012, 0.013, 0.014, 0.015, 0.016, 0.017, 0.018, 0.019 and 0.02m for the heat input of 2.51W. Fig. 8 also depicts the vapor volume fraction contour in (x-z) and (y-z) longitudinal middle planes. Since the tube is horizontally placed, the vapor volume fraction contour over the longitudinal middle plane of (y-z) is not symmetric and the volume fraction of the vapor in the upper part of the horizontal tube is higher due to gravity effects.

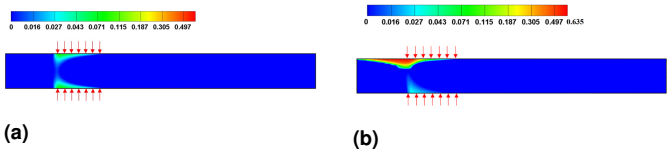

Fig. 8. Vapor volume fraction contour over the longitudinal middle planes: (a) x-z plane, (b) y-z plane.

Fig. **??** and Fig. 10 respectively show the axial velocity contour of the ferrofluid and the contour of the ferrofluid temperature at various transversal cross sections for the heat input of 2.51W. Due to the effects of gravity on the hydrodynamics of the induced two phase flow through the tube, the magnitude of the axial velocity of the induced flow through the tube in the upper part of the tube is lower than tube bottom.

Fig. 11 depicts the vapor volume fraction contours over the

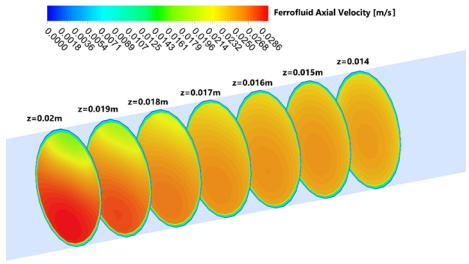

Fig. 9. Contour of the axial velocity of ferrofluid at different transversal cross sections for the heat input of 2.51W.

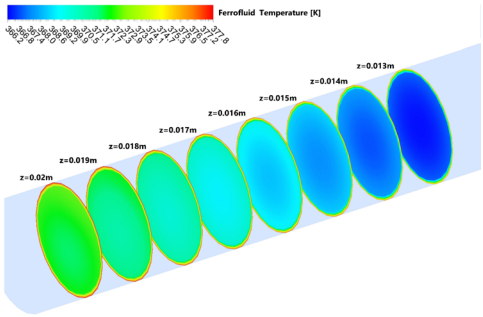

Fig. 10. Contour of the ferrofluid temperature at different transversal cross sections for the heat input of 2.51W.

transversal cross section of z=0.02m for different heat inputs of 1.76W, 2.01W, 2.26W and 2.51W. As seen, increasing the heat input has increased the vapor volume fraction.

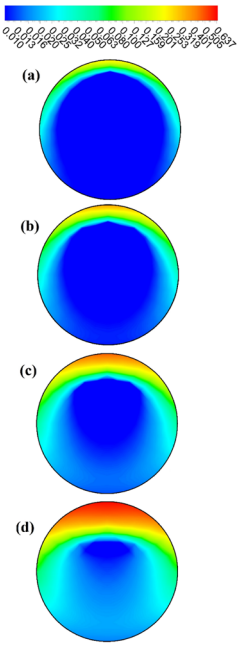

Fig. 11. Vapor volume fraction contours at the transversal cross section of z=0.02m for different heat inputs.

The nucleation site density and the vapor volume fraction in the heated region are shown in Fig. 12 and Fig. 13. As seen, with increase of distance from the start point of the heated region, more nucleation sites are activated and consequently the volume fraction of the vapor increases as well.

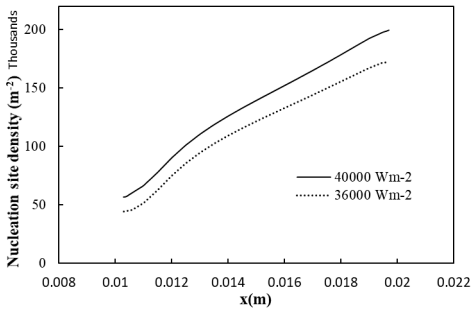

Fig. 12. Variations of the nucleation site density along the tube length in the heated region.

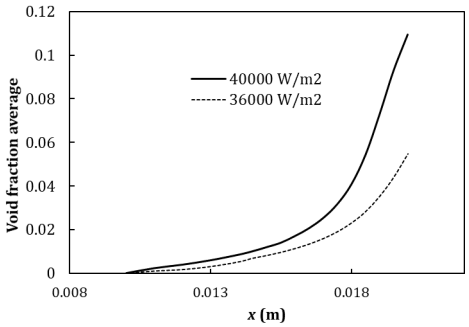

Fig. 13. Vapor volume fraction variations along the length of the tube in the heated region.

Fig. 14 shows how the local htc varies along the heated tube length in the heated region for the heat input of 2.51W. At the inlet of the heated region, the heat transfer by single-phase convection is the governing heat transfer mechanism. However, when the wall temperature exceeds the saturation temperature and reaches a certain value (as shown in Fig 15), subcooled flow boiling occurs and both nucleate boiling and single phase convection heat transfer are used to transfer heat from the wall. In the part of the tube where subcooled boiling heat transfer occurs, the wall temperature remains almost constant while the bulk temperature of the ferrofluid increases which results in considerable increase in htc along the heated section of the tube length due to subcooled flow boiling process.

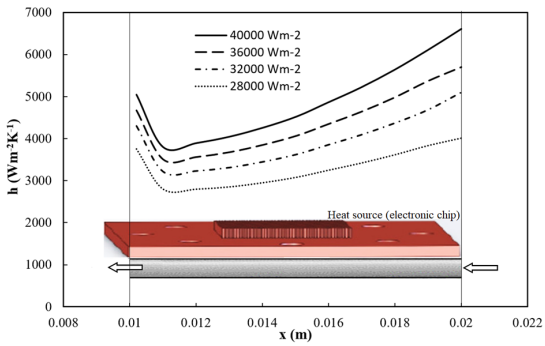

Fig. 14. Local htc variations along the tube length in the heated region.

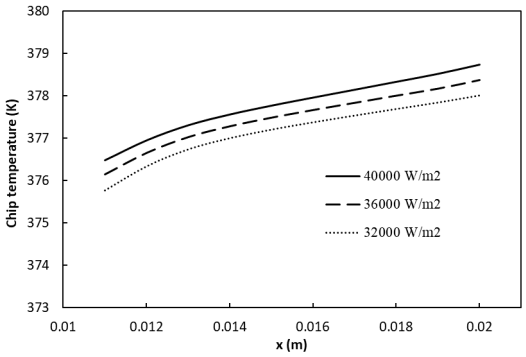

Fig. 15. Variations of the wall temperature (electronic chip temperature) along the tube length in the heated region.

Moreover, the boiling heat transfer (latent heat) is a key factor which can enhance the heat transfer of the magnetic fluid and a large amount of energy can be transported by phase change. Thus, the proposed magnetic-boiling induced heat transport device is not only able to pump the ferrofluid through the tube, but also is able to transfer a considerable amount of heat generated in the heat source as well.

Fig. 16 shows the variations of the average htc in the heated region for different applied heat inputs. As seen, by increasing the heat input, the driving magnetic force increases and the average htc increases as well. With the increase of heat input, the number of bubbles generated in the heated region increases, which will lead to a decrease in the magnetization of the fluid in this region. As a result, the magnetic force in this region which is a resisting force against the flow of the fluid decreases and the resulting magnetic force in the direction of the fluid movement increases, which contributes to increase of the velocity of the magnetic fluid flowing inside the pipe. With the increase of the fluid velocity inside the tube, the heat transfer coefficient of the flow over the heated surface will increase.

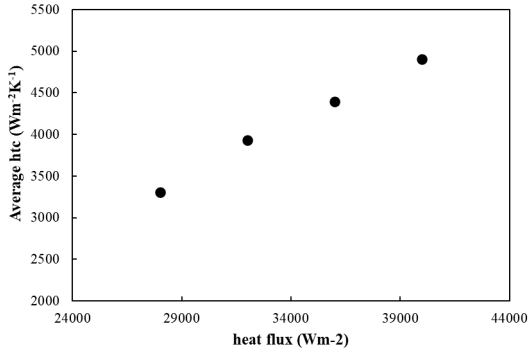

Fig. 16. Variations of the average htc in the heated region for different applied heat inputs.

Finally, as a suggestion, the proposed magnetic- boiling based pump can be used in a closed circulating loop as seen in Fig. 17, which consist a heat source and a cooling source (heat rejection) and it can transport a large amount of heat from heating section to the cooling section due to large latent heat of the boiling process. This cooling loop can extensively be used in electronics cooling applications. In such case, the heated ferrofluid is cooled in the cooling unit and the generated bubbles will be condensed.

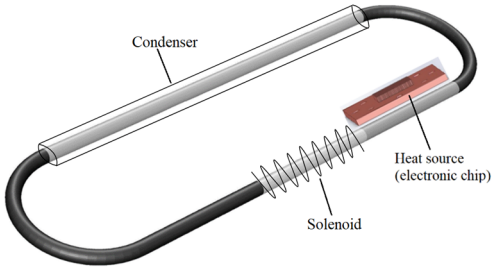

Fig. 17. Application of the proposed magnetic- boiling based pump in a closed circulating loop.

6. CONSLUSION

In the current paper, a magnetic-boiling driven heat transport device was simulated numerically and it represents a novel pumping system that can be operated by simply boiling and applying an external magnetic field which can transfer a considerable heat from the heat source. The technique of volume control and two fluid model were implemented for the numerical simulation of the proposed pump. The numerical results showed that the ferrofluid could be pumped inside a horizontal tube by applying MF accompanied by boiling of the ferrofluid and generation of vapors which contributes to reduction of the magnetization of the ferrofluid. The proposed pump can also transfer a considerable amount of heat from the heat source due to high htc of the boiling mechanism. Moreover, the results also revealed that with the increase of heat input, the number of bubbles generated in the heated region increases, which will lead to a decrease in the magnetization of the fluid in this region. As a result, the magnetic force in this region which is a resisting force against the flow of the fluid decreases and the resulting magnetic force in the direction of the fluid movement increases, which contributes to increase of the velocity of the magnetic fluid flowing inside the pipe.

REFERENCES

1. Y. Iwamoto, H. Yamaguchi, and X.-D. Niu, “Magnetically-driven heat transport device using a binary temperature-sensitive magnetic fluid,” *Journal of Magnetism and Magnetic Materials*, vol. 323, no. 10, pp. 1378–1383, 2011.
2. G. Karimi-Moghaddam, R. D. Gould, and S. Bhattacharya, “A nondimensional analysis to characterize thermomagnetic convection of a temperature sensitive magnetic fluid in a flow loop,” *Journal of Heat Transfer*, vol. 136, no. 9, 2014.
3. S. Kamiyama, T. Kamiya, and H. Izu, “Boiling two-phase flow characteristics of a magnetic fluid in-a nonuniform magnetic field. hiichiyo jibaka ni okeru jisei ryutai futto niso ryudo tokusei,” *Nippon Kikai Gakkai Ronbunshu, B Hen (Transactions of the Japan Society of Mechanical Engineers, Part B);(Japan)*, vol. 57, no. 537, 1991.
4. C.-C. Yang, J.-Y. Ji, C.-Y. Huang, Y. Ido, and Y. Iwamoto, “Experimental investigation of sub-millimeter thermomagnetic pumps with temperature-sensitive magnetic fluid,” *Applied Thermal Engineering*, vol. 219, p. 119461, 2023.
5. M. Pattanaik, V. Varma, S. Cheekati, G. Prasanna, N. Sudharsan, and R. Ramanujan, “A self-regulating multi-torus magneto-fluidic device for kilowatt level cooling,” *Energy Conversion and Management*, vol. 198, p. 111819, 2019.
6. S. Pal, A. Datta, S. Sen, A. Mukhopdhyay, K. Bandopadhyay, and R. Ganguly, “Characterization of a ferrofluid-based thermomagnetic pump for microfluidic applications,” *Journal of Magnetism and Magnetic Materials*, vol. 323, no. 21, pp. 2701–2709, 2011.
7. J. Tu and G. Yeoh, “On numerical modelling of low-pressure subcooled

boiling flows," *International Journal of Heat and Mass Transfer*, vol. 45, no. 6, pp. 1197–1209, 2002.
8. S. Ahangar Zonouzi, H. Safarzadeh, H. Aminfar, and M. Mohammadpourfard, "Experimental and numerical study of swirling subcooled flow boiling of water in a vertical annulus," *Experimental Heat Transfer*, vol. 31, no. 6, pp. 513–530, 2018.
9. M. Ishii and N. Zuber, "Relative motion and interfacial drag coefficient in dispersed two-phase flow of bubbles, drops and particles," *AIChE Journal*, vol. 25, no. 5, 1979.
10. A. Tomiyama, "Struggle with computational bubble dynamics," *Multiphase Science and Technology*, vol. 10, no. 4, pp. 369–405, 1998.
11. S. Antal, R. Lahey Jr, and J. Flaherty, "Analysis of phase distribution in fully developed laminar bubbly two-phase flow," *International journal of multiphase flow*, vol. 17, no. 5, pp. 635–652, 1991.
12. L. Ge, W. Wang, Z. Peng, F. Tan, X. Wang, J. Chen, and X. Qiao, "Facile fabrication of fe@ mgo magnetic nanocomposites for efficient removal of heavy metal ion and dye from water," *Powder Technology*, vol. 326, pp. 393–401, 2018.
13. N. Zuber, "On the dispersed two-phase flow in the laminar flow regime," *Chemical Engineering Science*, vol. 19, no. 11, pp. 897–917, 1964.
14. S. A. Zonouzi and A. Azizi, "Study of the magnetic taylor-couette flow with the axial flow in rotating machinery under quadrupole magnetic field," *Journal of Enhanced Heat Transfer*, vol. 30, no. 2, 2023.
15. A. R. Ahmadabadi, M. Rahimi, N. Azimi, and A. A. Alsairafi, "Natural convection heat transfer in an enclosure filled with fe 3 o 4 ferrofluid under static magnetic field: Experimental investigation and computational fluid dynamics modeling," *Journal of Enhanced Heat Transfer*, vol. 29, no. 1, 2022.
16. K. J. Buschow, *Handbook of magnetic materials*. Elsevier, 2003.
17. E. Solórzano, J. Reglero, M. Rodríguez-Pérez, D. Lehmhus, M. Wichmann, and J. De Saja, "An experimental study on the thermal conductivity of aluminium foams by using the transient plane source method," *International journal of heat and mass transfer*, vol. 51, no. 25-26, pp. 6259–6267, 2008.
18. N. Kurul, "On the modeling of multidimensional effects in boiling channels," *ANS. Proc. National Heat Transfer Con. Minneapolis, Minnesota, USA, 1991*, 1991.
19. V. H. Del Valle and D. Kenning, "Subcooled flow boiling at high heat flux," *International Journal of Heat and Mass Transfer*, vol. 28, no. 10, pp. 1907–1920, 1985.
20. M. Lemmert and J. Chawla, "Influence of flow velocity on surface boiling heat transfer coefficient," *Heat Transfer in Boiling*, vol. 237, no. 247, 1977.
21. N. Kurul, "On the modeling of multidimensional effects in boiling channels," *ANS. Proc. National Heat Transfer Con. Minneapolis, Minnesota, USA, 1991*, 1991.
22. V. Tolubinsky and D. Kostanchuk, "Vapour bubbles growth rate and heat transfer intensity at subcooled water boiling," in *International Heat Transfer Conference 4*, vol. 23, Begel House Inc., 1970.
23. T. Karayiannis, J. Lewis, D. Kenning, *et al.*, *Single-phase flow and flow boiling of water in horizontal rectangular microchannels*. PhD thesis, Brunel University School of Engineering and Design PhD Theses, 2013.
24. D. Kim, Y. Kwon, Y. Cho, C. Li, S. Cheong, Y. Hwang, J. Lee, D. Hong, and S. Moon, "Convective heat transfer characteristics of nanofluids under laminar and turbulent flow conditions," *Current Applied Physics*, vol. 9, no. 2, pp. e119–e123, 2009.
25. M. Bahiraei and M. Hangi, "Investigating the efficacy of magnetic nanofluid as a coolant in double-pipe heat exchanger in the presence of magnetic field," *Energy Conversion and Management*, vol. 76, pp. 1125–1133, 2013.
26. E. Manon, *Contribution à l'analyse et à la modélisation locale des écoulements bouillants sous-saturés dans les conditions des réacteurs à eau sous pression*. PhD thesis, Châtenay-Malabry, Ecole centrale de Paris, 2000.
27. J. Garnier, E. Manon, and G. Cubizolles, "Local measurements on flow boiling of refrigerant 12 in a vertical tube," *Multiphase Science and Technology*, vol. 13, no. 1&2, 2001.